

Optimized Zero-Watermarking Algorithm for Color Stereoscopic Images Based on OPCET

Chunpeng Wang^{1,2,*}, Guangze Li^{1,2}, Tingting Dai³, Dandan Han³

¹*Laboratory of Computing Power Network and Information Security, Ministry of Education, Shandong Computer Science Center, Qilu University of Technology (Shandong Academy of Sciences), Jinan, 250353, China*

²*Shandong Provincial Key Laboratory of Computer Networks, Shandong Fundamental Research Center for Computer Science, Jinan, 250353, China*

³*Shandong Qingcheng Digital Technology Co., Ltd., Jinan, 250353, China*

**Corresponding author*

Keywords: Color Stereoscopic Image; Octonion; PCET; Zero-Watermarking; Magnitude Optimization Strategy

Abstract: Color stereoscopic images have gained widespread attention due to their immersive experience in various applications. However, the accompanying issue of copyright protection has become increasingly prominent. Existing watermarking algorithms fail to effectively model the six-channel structure of color stereoscopic images (left-view R/G/B, right-view R/G/B), neglecting the intrinsic coupling relationships between viewpoints and color channels, resulting in limited robustness. To address this, this paper proposes a zero-watermarking algorithm for color stereoscopic images based on the Octonion Polar Complex Exponential Transform (OPCET) to achieve lossless copyright protection. Additionally, an optimization strategy for magnitude values is introduced to enhance the robustness and anti-attack capabilities of the watermark. Experimental results show that the proposed algorithm exhibits excellent robustness in multiple attack scenarios.

1. Introduction

With the continuous development of multimedia technology, stereoscopic images have become a key technology for providing immersive visual experiences in fields such as virtual reality, medical imaging, and 3D cinema. However, the issue of copyright protection has become increasingly severe. Embedded digital watermarking technology has become an effective means to address this problem by embedding invisible watermark information into image data to achieve copyright protection. However, during the watermark embedding process, embedded watermarking technology inevitably causes some damage to the original image, affecting its usability and quality. To solve this, zero-watermarking technology [1] has emerged. As a lossless watermarking technique, zero-watermarking does not modify the original image but generates watermark information related to the image, providing a new solution for copyright protection.

Image continuous orthogonal moments [2] are stable image features with strong anti-interference ability and geometric invariance. Applying them in zero-watermarking algorithms can significantly

enhance the algorithm's robustness against both conventional and geometric attacks. The zero-watermarking method based on image continuous orthogonal moments [3] has become mainstream in this field. However, applying these moments directly to stereoscopic image zero-watermarking algorithms faces three main problems:

The correlation between different viewpoints of stereoscopic images is ignored: Current IOMs are mainly applied to grayscale and color images, and their application to stereoscopic color images is relatively limited. Although multiple viewpoint images can be calculated separately, this method ignores the intrinsic coupling relationships between viewpoints and color channels, which disrupts the overall structure and integrity of the image, thus affecting the robustness of stereoscopic image zero-watermarking algorithms.

The problem of magnitude binarization in zero-watermark construction: The magnitude distribution of continuous orthogonal moments exhibits significant non-uniformity. The magnitude gradually decays as the moment order increases, leading to significant magnitude differences between lower-order and higher-order moments. This creates difficulties in achieving balanced information extraction during binarization, resulting in the over-amplification of low-order moments or the weakening, or even loss, of high-order moments. This imbalance in information extraction reduces the distinguishability of the zero-watermark and negatively impacts the algorithm's robustness.

To address these issues, the paper constructs an Octonion Polar Complex Exponential Transform (OPCET) suitable for color stereoscopic images, which describes the entire image while maintaining the intrinsic relationships between the channels and color components. The paper also introduces a magnitude optimization strategy for OPCET, which generates a more stable magnitude sequence and designs a zero-watermarking method for color stereoscopic images, resulting in improved robustness and resistance to geometric attacks.

The main contributions of this paper are as follows:

1) Based on octonion theory, this paper proposes an **Octonion Polar Complex Exponential Transform (OPCET)**, which enables the holistic processing of color stereoscopic images. By preserving the intrinsic correlations among all channels and color components (R/G/B from the left and right views), the method achieves high-dimensional feature representation of color stereoscopic images.

2) An **amplitude optimization strategy** for OPCET is proposed, upon which a zero-watermarking algorithm for color stereoscopic images is designed. By applying weighted optimization to the amplitude sequence, the proposed method significantly enhances the stability and robustness of the watermark features, while avoiding any modification to the image, thus ensuring a lossless copyright protection effect.

2. Continuous Orthogonal Moments for Images

2.1 Image Continuous Orthogonal Moments

Image continuous orthogonal moments are stable image features that have been widely used in multiple fields of image processing. These moments include Zernike Moments (ZMs) [4], Pseudo-Zernike Moments (PZMs) [5], Orthogonal Fourier-Mellin Moments (OFMMs) [6], Jacobi-Fourier Moments (JFMs) [7], Radial Harmonic Fourier Moments (RHFMs) [8], Polar Harmonic Fourier Moments (PHFMs) [9], and Polar Complex Exponential Transforms (PCTs, including PCET, PCT, and PST) [10]. These moments have been used for processing 2D grayscale images. However, with the development of image processing technologies, applications limited to grayscale images can no longer meet the practical needs of the field. Quaternion theory has provided a new approach for extending these methods to color images, and the series of quaternion

continuous orthogonal moments have become important tools for color image processing, including Quaternion Exponential Moments (QEMs) [11], Quaternion Polar Harmonic Transforms (QPHTs) [12], Quaternion Radial Harmonic-Fourier Moments (QRHFM) [13], and Quaternion Polar Harmonic-Fourier Moments (QPHFM) [14]. With the widespread use of 3D data in scientific research, stereoscopic images, as the core carriers of 3D information, have gained increasing importance in terms of feature extraction and analysis methods. To meet this need, special moment transformation methods for stereoscopic images have been proposed, including Ternary Radial Harmonic-Fourier Moments (TRHFM) [15], Ternary Polar Harmonic-Fourier Moments (TPHFM) [16].

2.2 Zero-Watermarking

Zero-watermarking is a non-embedding digital watermarking technology that does not modify the original image but generates watermark information based on the image's features. The robustness of zero-watermarking depends on the stability of the extracted features. According to the structure of the image features, zero-watermarking algorithms can be divided into three categories, (1) Spatial domain-based zero-watermarking algorithms: These algorithms are simple to compute and directly use image pixels to construct zero watermarks. They mainly include the LSB-based zero-watermarking algorithm [17] and the LBP-based algorithm [18], among others. However, they have poor robustness against noise, compression, and geometric attacks. (2) Transform domain-based zero-watermarking algorithms: These algorithms first perform a frequency domain transform on the image and then extract information suitable for constructing zero-watermarks. Due to the strong robustness and geometric invariance in the transform domain, they can handle attacks like JPEG compression, filtering, etc., although some methods may struggle with geometric attacks. They mainly include zero-watermarking algorithms based on Discrete Fourier Transform (DFT) [19], Discrete Cosine Transform (DCT) [20], Discrete Wavelet Transform (DWT) [21], and Lifting Wavelet Transform (LWT) [22], among others. (3) Zero-watermarking algorithms based on image continuous orthogonal moments: Since moments have rotational, scaling, and translation invariance, they are extremely robust against both conventional and geometric attacks. Methods based on Bessel-Fourier Moments [23], new types of Zernike Moments for zero-watermarking [4], and Fourier-Mellin Moments for color image zero-watermarking [24] have been developed, among others.

2.3 Stereoscopic Image Zero-Watermarking

Traditional zero-watermarking technologies are mainly designed for grayscale or color images and are difficult to adapt effectively to the multi-channel characteristics and inter-viewpoint correlation of stereoscopic images. As a result, researchers have proposed stereoscopic image zero-watermarking schemes to achieve lossless copyright protection and tampering detection for stereoscopic images. To further enhance robustness, researchers have introduced quaternion and octonion moment-based methods combined with continuous orthogonal moments to construct stereoscopic image zero-watermarks. Hypercomplex continuous orthogonal moments can represent both the left and right view information of stereoscopic images while providing geometric invariance, thereby enhancing the watermark's resistance to geometric attacks and signal processing attacks. The main methods include a stereoscopic image zero-watermarking scheme based on TRHFM [15], a TPCET-based zero-watermarking scheme [16], a TPHFM-based scheme [25], a dual-image robust watermarking method based on orthogonal Fourier–Mellin moments and chaotic mapping [26], a zero-watermarking scheme based on ORTM [27], and a stereoscopic image watermarking scheme based on OCOM [28]. These approaches not only fully exploit the global

features of stereoscopic images to enhance watermark robustness and stability but also offer more reliable solutions for copyright protection and integrity verification of stereoscopic images.

3. Octonion Polar Complex Exponential Transform

3.1 Definition of Polar Complex Exponential Transform

PCET [29] is a continuous orthogonal moment with strong feature description ability and geometric invariance, making it suitable for use as a stable image feature in various fields of digital image processing. For polar coordinate images, the PCET of order n and repetition m is defined as:

$$P_{nm} = \frac{1}{\pi} \int_0^{2\pi} \int_0^1 f(r, \theta) \overline{R_n(r)} \exp(\mathbf{j}m\theta) r dr d\theta \quad (1)$$

Basis function is defined as:

$$H_{nm}(r, \theta) = R_n(r) \exp(\mathbf{j}m\theta) \quad (2)$$

Here, $\overline{R_n(r)}$ denotes the conjugate of the radial basis function $R_n(r)$.

$$R_n(r) = \exp(\mathbf{j}2\pi nr^2) \quad (3)$$

It satisfies the following orthogonality condition:

$$\int_0^1 R_n(r) \overline{R_l(r)} r dr = \frac{1}{2} \delta_{nl} \quad (4)$$

To

$$\int_0^{2\pi} \int_0^1 R_n(r) \exp(\mathbf{j}m\theta) \overline{R_{n'}(r)} \exp(\mathbf{j}m'\theta) r dr d\theta = \pi \delta_{nn'} \delta_{mm'} \quad (5)$$

The PCET coefficient of an image $f(r, \theta)$ can be used to approximate the image, with higher-order moments providing better image reconstruction.

$$f(r, \theta) = \sum_{n=-\infty}^{+\infty} \sum_{m=-\infty}^{+\infty} P_{nm} R_n(r) \exp(\mathbf{j}m\theta) \quad (6)$$

3.2 Octonion Polar Complex Exponential Transform

PCET is only applicable to grayscale images and cannot handle color stereoscopic images. To address this limitation, we propose a method based on octonion theory, extending PCET from the complex number domain to the hypercomplex domain and introducing the Octonion Polar Complex Exponential Transform (OPCET). OPCET is capable of processing all the channels of a color stereoscopic image, preserving the interrelationships between the color components of the left and right views.

An octonion is an extension of complex numbers, with one real part and seven imaginary parts, as introduced by Baez et al. [30]. The octonion is represented as:

$$o = o_0 + o_1 e_1 + o_2 e_2 + o_3 e_3 + o_4 e_4 + o_5 e_5 + o_6 e_6 + o_7 e_7 \quad (7)$$

Where, o_0, o_1, \dots, o_7 represents 8 real numbers, and e_1, e_2, \dots, e_7 is the imaginary unit,

satisfying the properties of octonion [27].

If $o_0 \neq 0$, then the octonion o is a set of pure octonion. Based on the definition of octonion, we can represent the color stereoscopic image $f^o(r, \theta)$ as a set of pure octonion:

$$f^o(r, \theta) = f_{R1}^o(r, \theta)e_1 + f_{G1}^o(r, \theta)e_2 + f_{B1}^o(r, \theta)e_3 + f_{R2}^o(r, \theta)e_4 + f_{G2}^o(r, \theta)e_5 + f_{B2}^o(r, \theta)e_6 \quad (8)$$

Where, $f_1^o(r, \theta), f_2^o(r, \theta), \dots, f_6^o(r, \theta)$ these represent the R, B and G components of the left and right views of the color stereoscopic image.

$f^o(r, \theta)$ is the color stereoscopic image defined in polar coordinates. Since octonion multiplication does not satisfy the commutative property[31], and both $f^o(r, \theta)$ and $\exp(-\mu m \theta)$ are octonion, there are two ways to define the OPCET:

$$OP_{nm}^L = \frac{1}{\pi} \int_0^{2\pi} \int_0^1 \overline{R_n(r)} \exp(-\mu m \theta) f^o(r, \theta) r dr d\theta \quad (9)$$

$$OP_{nm}^R = \frac{1}{\pi} \int_0^{2\pi} \int_0^1 f^o(r, \theta) \overline{R_n(r)} \exp(-\mu m \theta) r dr d\theta \quad (10)$$

Where, $R_n(r) = \exp(\mu 2\pi n r^2)$, $\mu = \frac{1}{\sqrt{7}}(e_1 + e_2 + e_3 + \dots + e_7)$ is a pure octonion.

Since both $f^o(r, \theta)$ and $\exp(-\mu m \theta)$ are octonions, the resulting OPCET coefficients are also octonions. OPCET performs holistic processing of the multi-channel information in color stereoscopic images, preserving the coupling relationships among different channels and achieving a more effective representation of stereoscopic image content.

4. Zero-Watermarking Algorithm for Color Stereoscopic Images

4.1 Magnitude Optimization Strategy

The core of the zero-watermarking algorithm lies in extracting image features to construct the zero-watermark information. The stability of the features directly determines the robustness of the zero-watermarking algorithm. After obtaining the OPCET of the original image, stable magnitude sequences need to be selected to construct feature vectors. According to eq (5), n and m correspond to the frequency components of the image in the radial and angular directions. When n and m are smaller, the corresponding frequency components are lower. Since most of the image energy is typically concentrated in the low-frequency components, while high-frequency components often correspond to noise in the image, the magnitude for smaller n and m will be larger, and as n and m increase, the OPCET magnitude decreases.

A weight function is set to adjust the magnitude weights according to the increase in order n and repetition degree m . The weight function is defined as:

$$\omega_{nm} = \partial |n| + \beta |m| \quad (11)$$

Where ∂ and β beta are control parameters.

As the order $|n|$ and repetition degree $|m|$ increase, the weight increases, making the

higher-order amplitudes play a more significant role in the zero-watermark synthesis process. According to the test results from the dataset, the best effect is achieved when δ and β are both set to 0.5. Therefore, in subsequent experiments, we will set δ and β to 0.5 to ensure the optimization of the experimental data.

By introducing this weighting mechanism, higher-order amplitudes can play a more prominent role in the watermark embedding process, while the overall amplitude distribution becomes more balanced. Specifically, the selected stable amplitudes are multiplied by their corresponding weights to obtain the weighted amplitudes. The relationship between the weighted amplitude A_{nm}^{ω} and A_{nm} the original amplitude is expressed as:

$$A_{nm}^{\omega} = A_{nm} \times \omega_{nm} \quad (12)$$

Figure 1 shows the comparison of weighted magnitudes A_{nm}^{ω} and original magnitudes A_{nm} . As shown, after weighting, the magnitude distribution becomes more uniform, with higher-order magnitudes occupying a larger proportion, thus avoiding the situation where lower-order magnitudes dominate. This weighted optimization makes the magnitude distribution more balanced, providing more stable features for zero-watermark generation and verification.

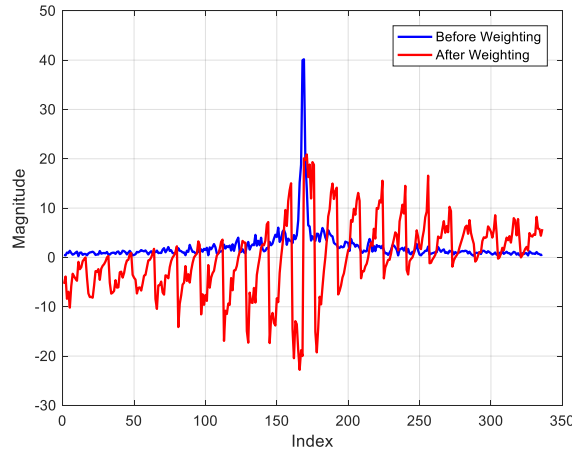


Figure 1: Comparison of weighted magnitudes versus original magnitudes (index n and m positions, with the center part (index value 168) corresponding to $(0, 0)$).

4.2 Zero-Watermark Generation and Verification

The zero-watermarking algorithm primarily consists of two steps: zero-watermark generation and zero watermark verification. Zero-watermark generation is mainly achieved by calculating the OPCET of the color stereoscopic image to construct the zero-watermark, while zero-watermark verification is used to confirm the copyright ownership of the image.

4.2.1 Zero-Watermark Generation Process

In the process of constructing a zero-watermark, the OPCET of the original image is first calculated. Then, an optimized amplitude sequence is obtained using a weighting mechanism. By expanding the amplitude sequence, a binary feature image is constructed. Finally, the binary feature image and the binary logo image are XORed to obtain the zero-watermark image. Assume that f^o is the original color stereoscopic image and L is a binary logo image of size $P \times Q$. The process

of constructing the zero-watermark is shown in Figure 2.

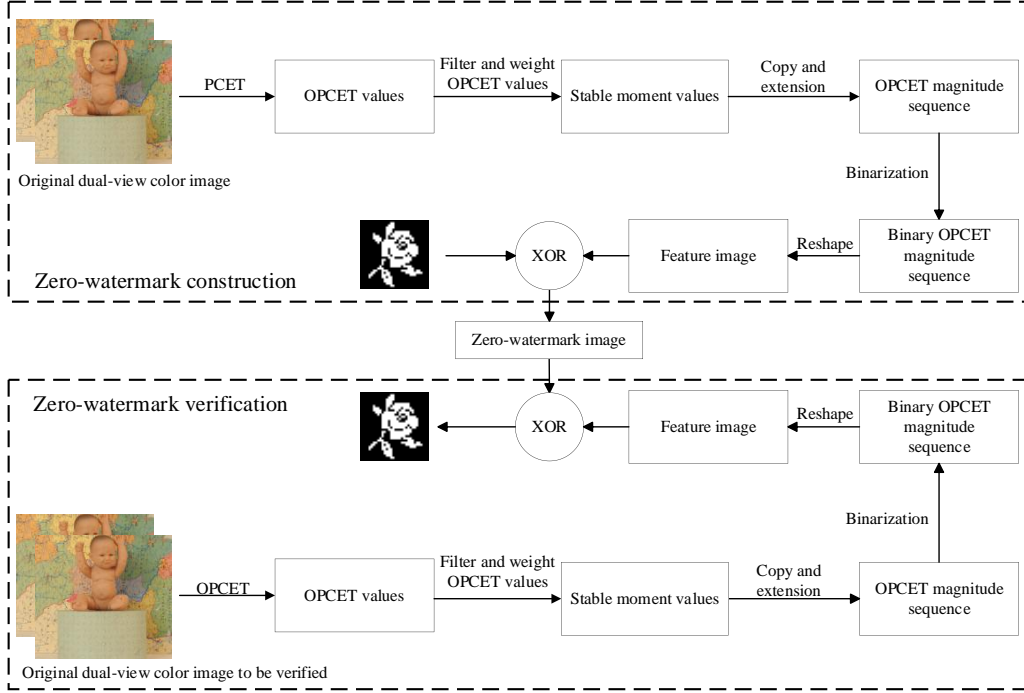


Figure 2: Flowchart of zero-watermarking algorithm

Calculating OPCET: Since high-order moments in image continuous orthogonal moments exhibit numerical instability, using high-order moments as image features for constructing zero-watermarks would negatively affect the performance of the zero-watermark algorithm. Thus, the algorithm only selects low-order moments to construct feature sequences. The OPCET of the original color stereoscopic image f^o is first calculated, and a sequence of moments A_{nm}^o is obtained, which includes $(2N_{\max} + 1)^2$ moment values. The corresponding magnitude sequence A is then derived

Optimizing the Magnitude Sequence: The weight mechanism is applied to A obtain a stable magnitude sequence $A^\omega = A \times \omega$.

Extending the Magnitude Sequence: The magnitude sequence A^ω is replicated several times to extend it to the $P \times Q$ size of the logo image, ensuring it aligns with the dimensions of the logo.

Binarizing the Magnitude Sequence: The magnitude sequence A is binarized to create a binary feature sequence E_b^ω .

$$E_b^\omega(i) = \begin{cases} 1, E^\omega(i) \geq T \\ 0, E^\omega(i) < T \end{cases} \quad (13)$$

Where T is the binarization threshold, which is set as the average value of E_b^ω .

Constructing Feature Image: The binary sequence E_b^ω is transformed into a higher-dimensional binary feature image F .

Generating Zero-Watermark Image: The logo image and the binary chaotic feature image F are XORed to obtain the zero-watermark image W .

$$W = XOR(L, F) \quad (14)$$

4.2.2 Zero-Watermark Verification Process

Calculating OPCET: The OPCET of the image $f^{o'}$ to be verified is calculated, obtaining the moment values $A_{nm}^{o'}$.

Optimizing the Magnitude Sequence: The magnitude sequence $A_{nm}^{o'}$ is selected and weighted A_{nm}' to obtain a stable magnitude sequence $A_{nm}^{\omega'} = A_{nm}' \times \omega_{nm}'$.

Extending the Magnitude Sequence: The stable magnitude sequence $A_{nm}^{\omega'}$ is replicated to match the $P \times Q$ size of the extended sequence $A' = \{a'(i), 0 \leq i < P \times Q\}$.

Binarizing the Magnitude Sequence: The magnitude sequence A' is binarized to form a binary feature sequence $A_b' = \{a_b'(i), 0 \leq i \leq P \times Q\}$.

$$a_b'(i) = \begin{cases} 1, a_b'(i) \geq T' \\ 0, a_b'(i) < T' \end{cases} \quad (15)$$

Where T' is the binarization threshold, which is set as the average value of A_b' .

Constructing Feature Image: The reassembled binary sequence A_b' is converted into a binary feature image $F' = \{f^{o'}(i, j), 0 \leq i < P, 0 \leq j < Q\}$.

Verifying the Zero-Watermark: The zero-watermark image W is XORed with the binary feature image F' to obtain a result image $L' = \{l'(i, j), 0 \leq i < P, 0 \leq j < Q\}$.

$$L' = XOR(W, F') \quad (16)$$

The Bit Consistency Rate (BCR) is used to measure the consistency between the detected image and the original image

$$BCR = \frac{C}{P \times Q} \times 100\% \quad (17)$$

5. Zero-Watermarking Experiment

5.1 Implementation Details

To comprehensively evaluate the performance of the proposed zero-watermarking method, we used the Middlebury Stereo Datasets, which contain 21 sets of color stereoscopic images of size 128×128 . A 32×32 binary image was used as the logo image. The maximum moment order was set to $N_{\max} = 10$. The simulation experiments were conducted using MATLAB R2016b on a personal computer with an Intel Core i7-4790 CPU, 32 GB of memory, and running the Microsoft Windows 10 operating system.

5.2 Robustness experiment

In this study, we introduced OPCET and optimized magnitude strategy to enhance the robustness and anti-attack capabilities of the watermark. To verify the superiority of the method, we compared it with other existing methods through extensive experiments. Kang et al. [32] proposed a flat image zero-watermarking algorithm based on PHTs and a 2D compound chaotic map. Wang et al. [31]

proposed a color stereoscopic image zero-watermarking algorithm based on octonion continuous orthogonal moments (OCOMs). Chu et al. [33] proposed a zero-watermarking algorithm for color images based on LWT-SVD and chaotic systems. Lu et al. [21] proposed a robust zero-watermarking algorithm for multi-medical images based on FFST-Schur and tent mapping.

Table 1: Robustness comparison

Attacks	proposed	algorithm[32]	algorithm[31]	algorithm[33]	algorithm[21]
M filtering 3×3	1	0.9818	0.9932	0.9927	1
M filtering 5×5	1	0.9804	0.9924	0.9914	0.9974
A filtering 3×3	1	0.9874	0.9916	1	1
A filtering 5×5	1	0.9740	0.9836	0.9827	0.9934
G filtering 3×3	1	0.9946	1	0.9970	0.9926
G noise 0.01	1	0.9470	0.9961	0.9876	0.9916
S & P noise 0.01	1	0.9544	0.9941	0.9865	0.9974
JPEG 30	1	0.9762	0.9912	1	1
Rotation 60°	0.9818	0.9860	0.9902	0.9837	0.9926
Scaling 0.5	1	1	0.9941	0.9929	0.9904
Scaling 1.5	1	1	0.9971	0.9944	0.9974
LWRC (0.5,1)	1	0.9901	0.9921	0.9923	1

By comparing the BCR values of each algorithm in Table 1, it is evident that the proposed method demonstrates significantly better robustness under various attacks than the other four algorithms. This indicates that the proposed algorithm not only exhibits superior geometric invariance, but also shows strong stability when handling complex attacks, thus achieving enhanced robustness.

6. Conclusion

This paper, based on the Polar Complex Exponential Transform (PCET) combined with octonion theory, constructs an OPCET suitable for color stereoscopic images, processes all the color components of the stereoscopic image while preserving the internal relationships between the channels. Furthermore, a weighted mechanism was introduced to optimize the magnitude sequence, successfully resolving the extreme magnitude issue and improving the stability and anti-attack capability of the zero-watermark. Experimental comparisons have validated the robustness of the OPCET in color stereoscopic image zero-watermarking. Future research could further explore other types of hypercomplex domain moment forms and more efficient optimization strategies to enhance the algorithm's applicability and performance, providing more comprehensive technical support for color stereoscopic image copyright protection.

References

- [1] Q. Wen, T. Sun, S. Wang, *Concept and application of zero-watermark*, *ACTA ELECTRONICA SINICA* 31 (2003) 214–216.
- [2] J. Yang, Z. Zeng, T. Kwong, Y.Y. Tang, Y. Wang, *Local Orthogonal Moments for Local Features*, *IEEE Transactions on Image Processing* 32 (2023) 3266–3280.
- [3] K. El-Khanchouli, H. Mansouri, N.E. Ghouate, H. Karmouni, N.-E. Joudar, M. Sayyouri, S.S. Askar, M. Abouhawwash, *Protecting Medical Images Using a Zero-Watermarking Approach Based on Fractional Racah Moments*, *IEEE Access* 13 (2025) 16978–17001.
- [4] H. Wang, Y. Chen, T. Zhao, *Modified Zernike Moments and Its Application in Geometrically Resilient Image Zero-Watermarking*, *Circuits, Systems, and Signal Processing* 41 (2022) 6844–6861.
- [5] D. Fu, X. Zhou, L. Xu, K. Hou, X. Chen, *Robust Reversible Watermarking by Fractional Order Zernike Moments and Pseudo-Zernike Moments*, *IEEE Transactions on Circuits and Systems for Video Technology* 33 (2023) 7310–7326.

- [6] C. Wang, L. Chen, Z. Xia, J. Li, Q. Li, Z. Wei, C. Wang, B. Han, *Novel Quaternion Orthogonal Fourier-Mellin Moments Using Optimized Factorial Calculation*, in: B. Ma, J. Li, Q. Li (Eds.), *Digital Forensics and Watermarking*, Springer Nature Singapore, Singapore, 2024: pp. 262–276.
- [7] J. Yang, X. Yuan, X. Lu, Y. Yan Tang, *Adjustable Jacobi–Fourier Moment for Image Representation*, *IEEE Transactions on Cybernetics* 55 (2025) 207–220.
- [8] H.-Y. Yang, X.-Y. Wang, P. Wang, P.-P. Niu, *Geometrically resilient digital watermarking scheme based on radial harmonic Fourier moments magnitude*, *AEU - International Journal of Electronics and Communications* 69 (2015) 389–399.
- [9] C. Wang, X. Wang, Z. Xia, B. Ma, Y.-Q. Shi, *Image description with polar harmonic fourier moments*, *IEEE Transactions on Circuits and Systems for Video Technology* 30 (2020) 4440–4452.
- [10] C. Wang, X. Wang, X. Chen, C. Zhang, *Robust zero-watermarking algorithm based on polar complex exponential transform and logistic mapping*, *Multimedia Tools and Applications* 76 (2017) 26355–26376.
- [11] X. Wang, Y. Liu, H. Xu, P. Wang, H. Yang, *Robust copy–move forgery detection using quaternion exponent moments*, *Pattern Analysis and Applications* 21 (2018) 451–467.
- [12] Y. Liu, S. Zhang, J. Yang, *Color image watermark decoder by modeling quaternion polar harmonic transform with BKF distribution*, *Signal Processing: Image Communication* 88 (2020) 115946.
- [13] T. Sheng, W. Zeng, B. Yang, C. Fu, *Adaptive multiple zero-watermarking based on local fast quaternion radial harmonic Fourier moments for color medical images*, *Biomedical Signal Processing and Control* 86 (2023) 105304.
- [14] S. Yang, A. Deng, *Quaternion fast and accurate polar harmonic Fourier moments for color image analysis and object recognition*, *J. Opt. Soc. Am. A* 41 (2024) 852–862.
- [15] C. Wang, X. Wang, Z. Xia, C. Zhang, *Ternary radial harmonic Fourier moments based robust stereo image zero-watermarking algorithm*, *Information Sciences* 470 (2019) 109–120.
- [16] B. Ma, L. Chang, C. Wang, J. Li, G. Li, Z. Xia, X. Wang, *Double Medical Images Zero-Watermarking Algorithm Based on the Chaotic System and Ternary Accurate Polar Complex Exponential Transform*, *Journal of Mathematical Imaging and Vision* 63 (2021) 1160–1178.
- [17] E. Elbasi, V. Kaya, *Robust Medical Image Watermarking Using Frequency Domain and Least Significant Bits Algorithms*, in: *2018 International Conference on Computing Sciences and Engineering (ICCSE)*, 2018: pp. 1–5.
- [18] H. Shi, S. Zhou, M. Chen, M. Li, *A novel zero-watermarking algorithm based on multi-feature and DNA encryption for medical images*, *Multimedia Tools and Applications* 82 (2023) 36507–36552.
- [19] M. Cedillo-Hernandez, F. Garcia-Ugalde, M. Nakano-Miyatake, H. Perez-Meana, *Robust watermarking method in DFT domain for effective management of medical imaging*, *Signal, Image and Video Processing* 9 (2015) 1163–1178.
- [20] S.A. Nawaz, J. Li, M.U. Shoukat, U.A. Bhatti, M.A. Raza, *Hybrid medical image zero watermarking via discrete wavelet transform-ResNet101 and discrete cosine transform*, *Computers and Electrical Engineering* 112 (2023) 108985.
- [21] Y. Lu, X. Lu, G. Yang, X. Xiong, *Robust zero-watermarking algorithm for multi-medical images based on FFST-Schur and Tent mapping*, *Biomedical Signal Processing and Control* 96 (2024) 106557.
- [22] S. Kahdim, A. Abduldaim, *Zero watermarking technique using LWT*, *International Journal of Nonlinear Analysis and Applications* 14 (2023) 2399–2407.
- [23] G. Gao, G. Jiang, *Bessel-Fourier moment-based robust image zero-watermarking*, *Multimedia Tools and Applications* 74 (2015) 841–858.
- [24] Z. Shao, Y. Shang, R. Zeng, H. Shu, G. Coatrieux, J. Wu, *Robust watermarking scheme for color image based on quaternion-type moment invariants and visual cryptography*, *Signal Processing: Image Communication* 48 (2016) 12–21.
- [25] C. Wang, B. Ma, Z. Xia, J. Li, Q. Li, Y.-Q. Shi, *Stereoscopic Image Description With Trinion Fractional-Order Continuous Orthogonal Moments*, *IEEE Transactions on Circuits and Systems for Video Technology* 32 (2022) 1998–2012.
- [26] Z. Shao, Y. Shang, Y. Zhang, X. Liu, G. Guo, *Robust watermarking using orthogonal Fourier–Mellin moments and chaotic map for double images*, *Signal Processing* 120 (2016) 522–531.
- [27] M. Yamni, H. Karmouni, M. Sayyouri, H. Qjidaa, J. Flusser, *Novel Octonion Moments for color stereo image analysis*, *Digital Signal Processing* 108 (2021) 102878.
- [28] C. Wang, Q. Hao, B. Ma, X. Wu, J. Li, Z. Xia, H. Gao, *Octonion continuous orthogonal moments and their applications in color stereoscopic image reconstruction and zero-watermarking*, *Engineering Applications of Artificial Intelligence* 106 (2021) 104450.
- [29] Z. Yang, L. Yang, G. Chen, P.-T. Yap, *Improved polar complex exponential transform for robust local image description*, *Pattern Recognition* 143 (2023) 109786.
- [30] W.-J. Zhou, M. Yu, S.-M. Yu, *A zero-watermarking algorithm of stereoscopic image based on hyperchaotic system*, *Acta Physica Sinica* 61 (2012) 117–126.
- [31] C. Wang, Q. Hao, B. Ma, X. Wu, J. Li, Z. Xia, H. Gao, *Octonion continuous orthogonal moments and their applications in color stereoscopic image reconstruction and zero-watermarking*, *Engineering Applications of Artificial*

Intelligence 106 (2021) 104450.

[32] X. Kang, F. Zhao, Y. Chen, G. Lin, C. Jing, Combining polar harmonic transforms and 2D compound chaotic map for distinguishable and robust color image zero-watermarking algorithm, *Journal of Visual Communication and Image Representation* 70 (2020) 102804.

[33] R. Chu, S. Zhang, J. Mou, X. Gao, A zero-watermarking for color image based on LWT-SVD and chaotic system, *Multimedia Tools and Applications* 82 (2023) 34565–34588.